Pediatric Ovarian Torsion: Spectrum of Imaging Findings[1]

Akosua Sintim-Damoa, MD
Anand Shyamcharan Majmudar, MD
Harris L. Cohen, MD
Louis Swig Parvey, MD

RadioGraphics 2017; 37:1892–1908

https://doi.org/10.1148/rg.2017170026

Content Codes: GU PD US

[1]From the Department of Radiology, LeBonheur Children's Hospital, University of Tennessee Health Science Center, 848 Adams Ave, Memphis, TN 38103. Presented as an education exhibit at the 2016 RSNA Annual Meeting. Received February 23, 2017; revision requested May 25 and received June 23; accepted June 27. For this journal-based SA-CME activity, the authors, editor, and reviewers have disclosed no relevant relationships. **Address correspondence to** A.S.D. (e-mail: *asintimd@uthsc.edu*).

SA-CME LEARNING OBJECTIVES

After completing this journal-based SA-CME activity, participants will be able to:

- Name three factors that contribute to ovarian torsion in the pediatric population.
- Describe three US findings of ovarian torsion seen in adolescents.
- List three imaging patterns of ovarian torsion seen in neonates.

See www.rsna.org/education/search/RG.

The accurate diagnosis of ovarian torsion is imperative, as loss of the ovary can have long-term consequences in terms of fertility. However, a nonspecific clinical presentation in conjunction with a highly variable imaging appearance makes the diagnosis of ovarian torsion challenging. This is complicated even further in the pediatric population, as these patients cannot always articulate their symptoms or provide an adequate medical history. Therefore, imaging has a critical role in the diagnosis of ovarian torsion in pediatric patients. Common imaging findings of ovarian torsion in the prepubescent and adolescent populations include asymmetric enlargement of the ovary, peripheral location of ovarian follicles, and midline location of the ovary. A coexistent mass within the ovary may or may not be present. Antenatal torsion also can occur and may be discovered at routine or specific imaging of the fetus or postnatal imaging of the neonate. Imaging findings in the perinatal population that may suggest torsion include a cystic mass with a fluid-debris level and a complex, multiseptated mass. This article reviews ovarian torsion throughout the pediatric years—from the fetal period through adolescence. It reviews the clinical presentation and imaging findings of this abnormality while describing the relevant anatomy, embryologic features, and pathophysiology. Ovarian torsion may be variable in appearance owing to the age and degree of torsion, which is seen early as a large ovary with peripheral follicles and later, once necrosis has ensued, as a complex cystic mass.

Introduction

Ovarian torsion is a surgical emergency that can lead to impaired or lost fertility if the diagnosis and intervention are delayed. Ovarian torsion refers to complete or partial twisting of the vascular pedicle in the suspensory ligament, leading to obstructed lymphatic flow followed by obstructed venous flow and finally obstructed arterial flow. Without surgical intervention, the ovary may be lost; therefore, the diagnosis is important. However, rendering an accurate diagnosis of ovarian torsion is challenging. The clinical findings are nonspecific and may be simulated by those of several other emergent abdominopelvic pathologic conditions. Rendering the

TEACHING POINTS

- The most commonly described finding of ovarian torsion in children and adolescents is an enlarged ovary on US images, which may appear solid with early torsion or heterogeneous or echoless with later torsion, particularly if there is necrosis.
- Comparing the size of the ovary of concern with the size of the contralateral ovary is key to making an accurate diagnosis of ovarian torsion.
- A specific US sign described in association with ovarian torsion in adolescents is the presence of multiple follicles at the periphery of a unilaterally enlarged edematous ovary.
- Color Doppler US evaluation is not reliable for confirming or excluding ovarian torsion.
- A fluid-debris level in an ovarian cyst is a specific sign of ovarian torsion in neonates and secondary to cyst fluid separating from a liquefied hematoma.

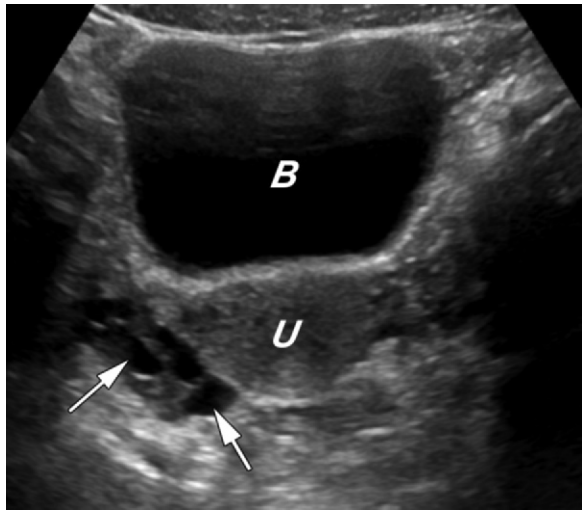

Figure 1. Normal ovary in a 16-year-old girl. Transverse gray-scale US image shows a normal ellipsoid right ovary with anechoic follicles (arrows) randomly distributed throughout the parenchyma. *B* = urinary bladder, *U* = uterus.

diagnosis is more difficult in the younger pediatric population than in teens and adults because these patients often cannot clearly communicate their symptoms. Owing to the nonspecific clinical picture, many clinicians rely on imaging, ultrasonography (US) in particular, in making the diagnosis of ovarian torsion. The aim of this article is to describe the imaging findings of ovarian torsion throughout the pediatric years, from the fetal period through adolescence. It is essential for radiologists to correlate the clinical and imaging findings and maintain a high index of suspicion to correctly diagnose ovarian torsion.

Epidemiology Features and Clinical Presentations

Fifteen percent of all ovarian torsions occur in the pediatric population (1–3). Although ovarian torsion can be seen in pediatric patients of all ages, from infancy through adolescence, in the pediatric population, the peak incidence occurs during early adolescence and the immediate postmenarchal years (2,4–6). In a study of 97 cases of pediatric ovarian torsion (3,4), 48 (50%) of the cases occurred in girls between 9 and 14 years of age. Two distinct peaks in the age distribution of pediatric ovarian torsion have been reported, with one peak occurring in infants and the other occurring at 12 years of age (3,4). Although isolated fallopian tube torsion can occur in adolescents and ovulating women, it is very rare, with an incidence of one in 1.5 million females (7).

Patients with ovarian torsion may present with sudden acute lower abdominal pain, nausea, vomiting, fever, or dysuria (2,5,8,9). Leukocytosis may be noted (5). Alternatively, patients can have a subacute presentation, with days or weeks of episodic pelvic pain (5,8). Patients exhibiting "waves" of acute pelvic pain with nausea may be experiencing intermittent ovarian torsion (5). A substantial number (16%) of cases of pediatric ovarian torsion occur in persons younger than 1 year, in whom there is limited ability to assess for pain (4). Ovarian torsion can be seen in newborns, who may be asymptomatic but were found to have abnormal prenatal US findings (10). Affected neonates may present with an abdominal mass or feeding intolerance (10).

Embryologic Features and Anatomy

In the absence of a Y chromosome, the primitive gonad does not differentiate into the ovary until the 10th week of embryonic life (11). By 16 weeks, ovarian primordial follicles develop (11). The ovaries begin their development at the level of the 10th thoracic vertebrae along the posterior abdominal wall (12). As the ovaries mature, they descend into the pelvis, and by puberty, they are lateral in the true pelvis at the level of the broad ligament (12,13). They are oval structures that are normally posterior or lateral to the uterus and medial and anterior to the iliac vessels by the time of menarche, but they may be present anywhere along their embryologic course (14) (Figs 1, 2). At times, the ovaries may herniate into the canal of Nuck and can be found in an inguinal location. They have a dual arterial supply from the ovarian arteries by way of the abdominal aorta and from the ascending branches of the uterine arteries by way of the internal iliac artery (15). The ovarian arteries are relatively short early in intrauterine life, when they flank the vertebral column inferior to the kidneys; they gradually lengthen as the ovaries

Figure 2. Normal ovary in a 17-year-old girl with an absent uterus. Coronal T2-weighted magnetic resonance (MR) image shows the left ovary (arrow) high in the pelvis. The ovary can be identified by its multiple round hyperintense follicles. Its position at the level of the superior iliac bone is not uncommon but would make analysis with use of the transvaginal technique more limited.

descend into the pelvis (15). The right ovarian vein drains directly into the inferior vena cava, whereas the left ovarian vein drains first into the left renal vein and then into the inferior vena cava (15).

The ovary is composed of an outer cortex and an inner medulla. The cortex is thicker than the medulla and contains numerous follicles separated by stromal tissue. Follicles may be seen in girls of all ages (13,16).

The ovarian volume is affected by the girl's age and pubertal status (17,18). The volume of the ovary can be calculated by using the formula for a prolate ellipsoid: length × width × height × 0.523. During the first 3 months of life, gonadotropin levels increase abruptly secondary to the decrease in neonatal estrogen and progesterone levels that results after separation of the newborn from the placenta (14,18,19). The mean ovarian volume in infants up to 3 months of age is 1.06 cm^3 and can be as high as 3.6 cm^3 (20). The mean ovarian volume has been reported as 1.05 cm^3 in girls 4–12 months old and 0.67 cm^3 in girls 13–24 months old (20). In premenarchal girls 2–13 years of age, the mean ovarian volume is 0.7–4.2 cm^3 (13). The mean ovarian volume is approximately 9.8 cm^3 in menstruating females (13).

Pathophysiology

Torsion of the vascular pedicle leads first to impaired lymphatic outflow and subsequently to diminished venous outflow from the ovary. Ovarian engorgement and edema ensue and lead to increased pressure within the ovary. Without intervention, the arterial blood supply is compromised and eventually leads to ovarian infarction.

Pediatric ovarian torsion can occur in the setting of an adnexal mass or cyst, or it may result from torsion of a normal ovary (4,21). In several large studies of pediatric ovarian torsion (4,9,22), the prevalence of an underlying adnexal pathologic condition was 51%–84%. The most frequently encountered adnexal lesions are mature cystic teratomas and follicular cysts (4,9,22). Malignancy in a torsed adnexal mass is extremely rare (22).

The presence of large adnexal cysts can predispose the ovary to torsion (9). Functional ovarian cysts in children usually develop as a result of hormonal stimulation (9,22). Hormonal stimulation of the ovary occurs during two peak periods: the 1st year of life and at menarche (4,9,22). Antenatal cases of ovarian torsion are probably related to maternal hormonal influence (14,18). Under the influence of maternal hormones, the fetal ovary enlarges and can develop cysts, which may predispose the ovary to torsion (3,4). During menarche, ovarian enlargement and cyst formation occur in response to a maturing hypothalamic-pituitary-gonadal axis (4,9,12,22). During the 1st months after menarche, 20% of girls may have enlarged ovaries with multiple cysts, the majority of which involute (9,22). The results of several studies have shown that the risk of torsion correlates with cyst size and is greater when cysts measure 4–5 cm (22–25).

Torsion of normal adnexa also can occur and is more common in the pediatric population than in adults (2,21). Torsion of the normal ovary is attributed to the increased mobility and tortuosity of the adnexa in girls, which allow ease of ligamentous twisting (2,3,21,26). In girls, the ovarian ligaments, which contain the ovarian vessels, may be long owing to the incomplete descent of the ovaries from the abdomen into the pelvis (12,15). The descent is usually complete by early puberty (12,13,15). Ovarian torsion is uncommon after pelvic inflammatory

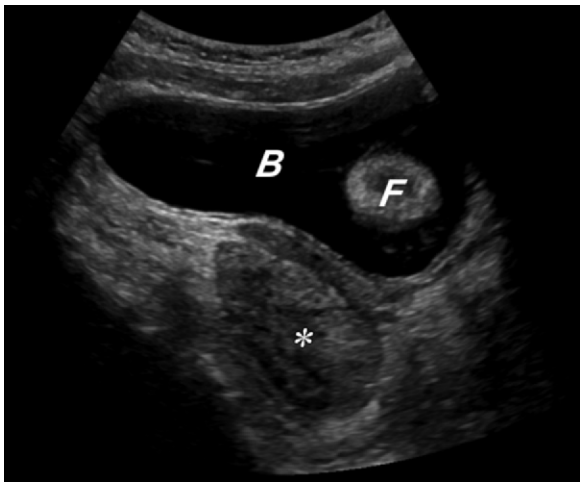

Figure 3. Ovarian torsion in a 9-year-old girl who presented with sudden-onset right lower quadrant pain. Sagittal gray-scale US image shows an enlarged, solid-appearing midline right ovary (*) with no definable follicles. The volume of the right ovary was 34 cm^3. Ovarian torsion was confirmed at surgery. *B* = urinary bladder, *F* = Foley catheter balloon.

disease, during which adhesions can restrict the movement of the adnexa (27).

Imaging

The primary modality for imaging the ovaries during the acute manifestion of torsion is US, which is readily available and does not require the use of ionizing radiation. The bladder is used as the sonographic window and is distended by means of oral fluid intake or bladder catheterization. A distended bladder displaces the small bowel loops superiorly, out of the pelvis (14). US is performed by using a transducer of the highest frequency possible for the given body habitus. The ovaries typically appear adjacent to the uterus when the region is scanned in the transverse plane while angling the transducer superiorly and inferiorly. The normal ovary can be identified by its oval shape and randomly distributed anechoic round follicles, which distinguish it from bowel (Figs 1, 2). US evaluation of the ovaries can be more challenging in the pediatric population than in adults. The ovaries of pediatric patients can be small and difficult to identify. Also, owing to the relatively shallow pelvis in neonates and very young infants, their ovaries may not be found in the pelvis but rather in a more cranial position within the lower region of the abdomen—especially if they are associated with a mass. Although transvaginal imaging is useful in the adult population for more detailed evaluation of the ovaries, it is relatively contraindicated for virginal patients and therefore not commonly performed in the pediatric population (17,28).

Color Doppler US can be used to detect flow within the ovaries, but it cannot be used to differentiate blood flow from the uterine and ovarian arteries. Siegel and Quillin (13,29) reported that color Doppler flow can be seen in 80% of prepubertal ovaries and 90% of postmenarchal ovaries at transabdominal imaging.

Table 1: Imaging Patterns of Ovarian Torsion in Children and Adolescents

Enlarged ovary
Solid mass
Solid mass with peripheral cysts
Cystic mass
Midline location of ovary
Free fluid in the pelvis
Adnexal/paraovarian cyst or mass

Imaging Patterns in Children and Adolescents

The ovarian morphology is key to the diagnosis of ovarian torsion. Torsed ovaries have a variable appearance related to the degree of internal hemorrhage, stromal edema, infarction, and necrosis that has occurred by the time they are imaged (14). The most consistently seen imaging feature of ovarian torsion in children and adolescents is unilateral ovarian enlargement (2,3,13,14,17,21,30) (Table 1). The enlarged ovary may appear as a solid structure or as a solid structure with peripheral cysts, a finding likened to a string of pearls (2,5,30–32) (Figs 3–7). This enlargement, and in some cases increased echogenicity, of the ovary is thought to be secondary to stromal edema and hemorrhage. The normal US appearance of the ovary is lost, with follicles no longer appearing randomly distributed throughout the ovarian parenchyma but rather appearing at the periphery of the ovary or not visible at all. Necrotic ovaries may appear as more complex or cystic structures, having lost their parenchyma (Figs 7, 8). Other nonspecific findings that are sometimes seen with ovarian torsion in children and adolescents include an atypical position of the ovary in the pelvis, particularly when seen in the midline or contralateral pelvis, free fluid in the pelvis, and adnexal masses or cysts. In addition, several studies have shown a right-sided predominance of ovarian torsion, with a right side–to–left side predominance ratio of 3:2 (2,4). This has been attributed to the relative mobility of the cecum, which allows greater movement of the right ovary, and the fixed position of the sigmoid colon, which limits movement of the left ovary (4). With acute ovarian torsion, there can be tenderness of the ovary with probe palpation at US (3,27).

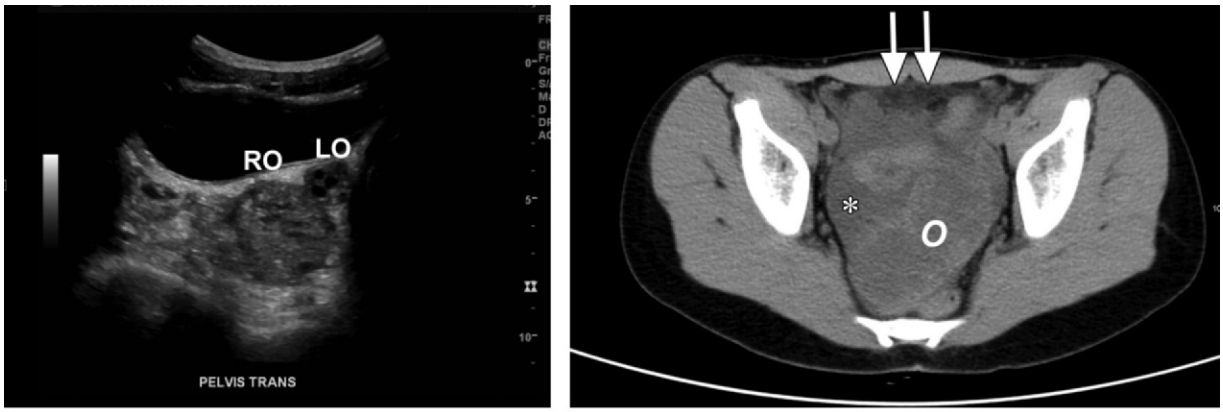

Figure 4. Ovarian torsion in a 14-year-old girl. **(a)** Transverse gray-scale US image shows an enlarged, predominantly solid-appearing torsed right ovary *(RO)* in the midline posterior to the bladder. Physiologic follicles are seen in the normal small left ovary *(LO)*. The volume of the right ovary is 25 times greater than that of the left ovary. The surgically proven diagnosis was ovarian torsion. **(b)** Axial non–contrast material–enhanced computed tomographic (CT) image of the pelvis shows a midline to left-sided mass *(O)* with predominantly central low attenuation, consistent with a torsed right ovary. Free fluid (∗) and increased attenuation of the anterior pelvic fat (arrows) also are seen.

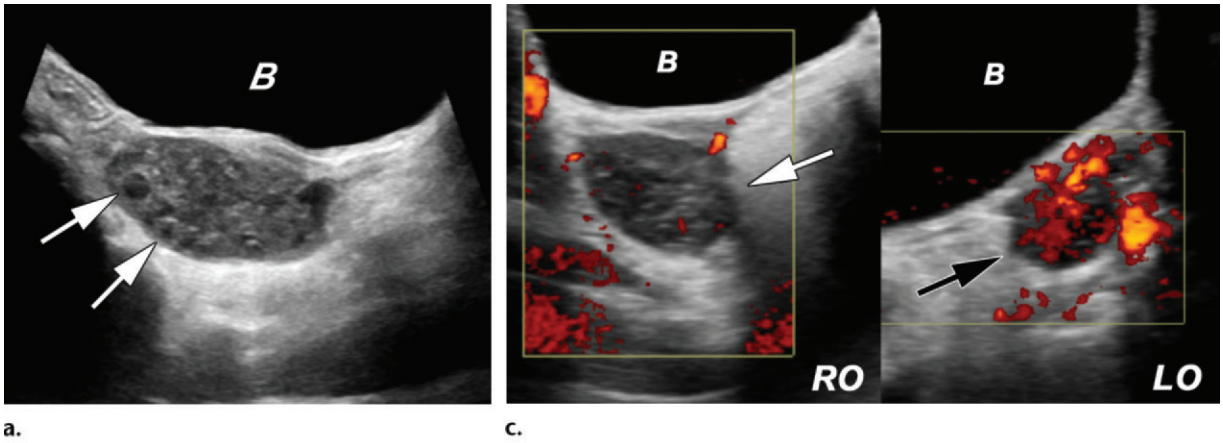

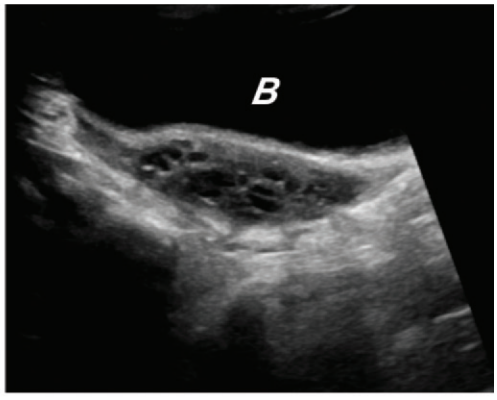

Figure 5. Ovarian torsion in a 6-year-old girl with right lower quadrant pain and vomiting. *B* = urinary bladder. **(a)** Sagittal gray-scale US image shows prominent peripheral follicles (arrows) in an enlarged right ovary with a volume of 15.3 cm^3. **(b)** Sagittal gray-scale US image shows normal follicles interspersed within a normal left ovary, which has a volume of 6.4 cm^3. **(c)** Transverse power color Doppler US images of the right ovary (*RO,* white arrow) and left ovary (*LO,* black arrow) show relatively decreased flow in the right ovary compared with the flow seen in the contralateral ovary. Right ovarian torsion was found at surgery.

Ovarian Enlargement.—The most commonly described finding of ovarian torsion in children and adolescents is an enlarged ovary on US images, which may appear solid with early torsion or heterogeneous or echoless with later torsion, particularly if there is necrosis (2,3,13,14,17,21,30). When determining whether an ovary is enlarged, comparison of the ovarian volume with established normal values for the various stages of childhood is extremely important. Noting that the typical expected ovarian volume for a premenarchal child is 1–2 cm^3, in the appropriate clinical scenario, one must be concerned when the ovarian volume is 6–8 cm^3 or greater, which is at least three to four times the normal volume (20,33). In teenagers, the mean ovarian volume is 6–9 cm^3, with normal volumes as large as 22 cm^3 (33). In this population, ovarian volumes of 45–60 cm^3 should raise concern for torsion (33). Ovarian volumes are highly variable among children of different ages and depend in part on the hormonal

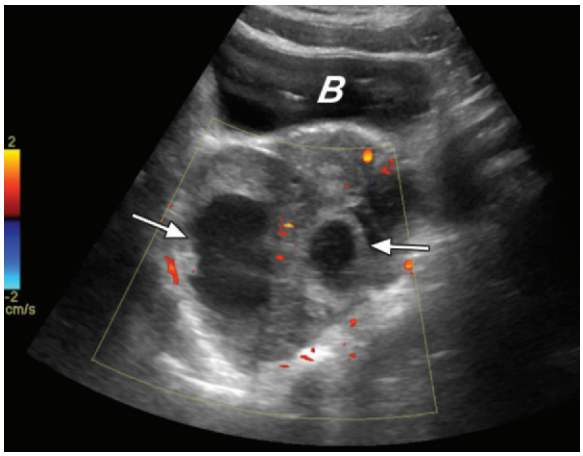

Figure 6. Ovarian torsion in a 16-year-old girl with right lower quadrant pain of 2 days' duration. Transverse color Doppler US image of the pelvis shows an enlarged right ovary with a volume of 348 cm^3. Large peripheral cysts (arrows) also are seen. *B* = urinary bladder.

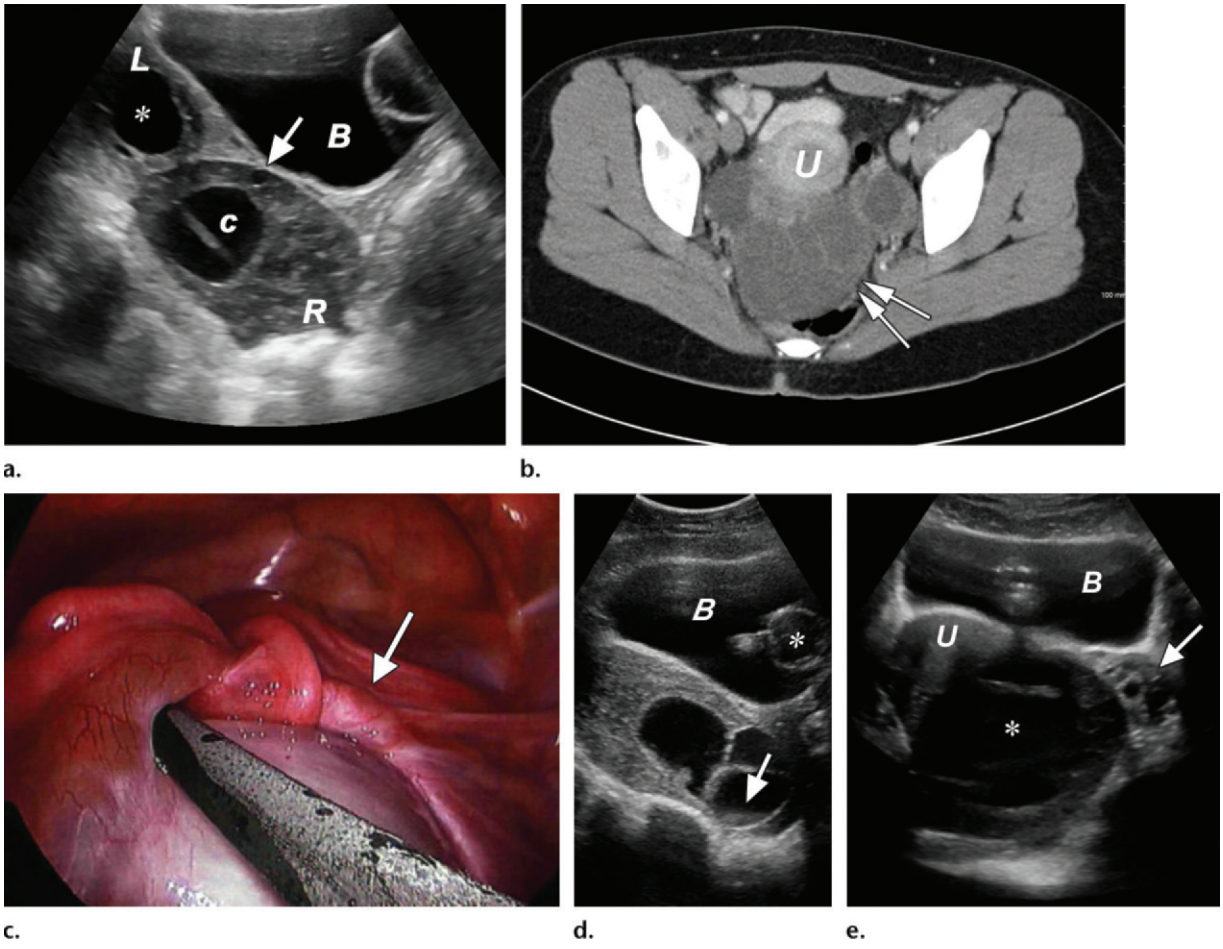

Figure 7. Ovarian torsion in a 15-year-old girl with pain, vomiting, and a history of recurrent ovarian torsions during a 2-year period. **(a)** Sagittal pelvic US image obtained during the initial emergency department visit shows that the right ovary *(R)* is markedly enlarged compared with the left ovary *(L)* and contains a prominent cyst *(c)* with a septation. A small peripheral follicle (arrow) is seen in the right ovary, and a simple cyst (*) is seen in the left ovary. This image was obtained by orienting the transducer in the sagittal plane over the left pelvis and angling inferiorly to use the bladder *(B)* as a sonographic window and thus allow better visualization of the abnormal right ovary. **(b)** Axial contrast-enhanced pelvic CT image obtained the same day as **a** shows a low-attenuating midline mass (arrows), which is the torsed ovary, posterior to and to the left of the uterus *(U)*. The torsed ovary contains enlarged cysts and has poor contrast enhancement. **(c)** Intraoperative photograph shows twisting of the pedicle of the right adnexum (arrow). The patient was treated with surgical detorsion. **(d)** Sagittal US image obtained 2 years later, when the patient was aged 17 years, shows an enlarged right ovary with several prominent cysts and follicles. One follicle contains a fluid-debris level (arrow). A Foley catheter balloon (*) is seen in the urinary bladder *(B)*. Surgical detorsion and oophoropexy were performed. **(e)** Transverse pelvic US image obtained 2 months after **d** shows that the right ovary (*) is still enlarged, with cysts replacing the majority of the parenchyma. The left ovary (arrow) is normal. The patient was treated with right oophorectomy. *B* = bladder, *U* = uterus.

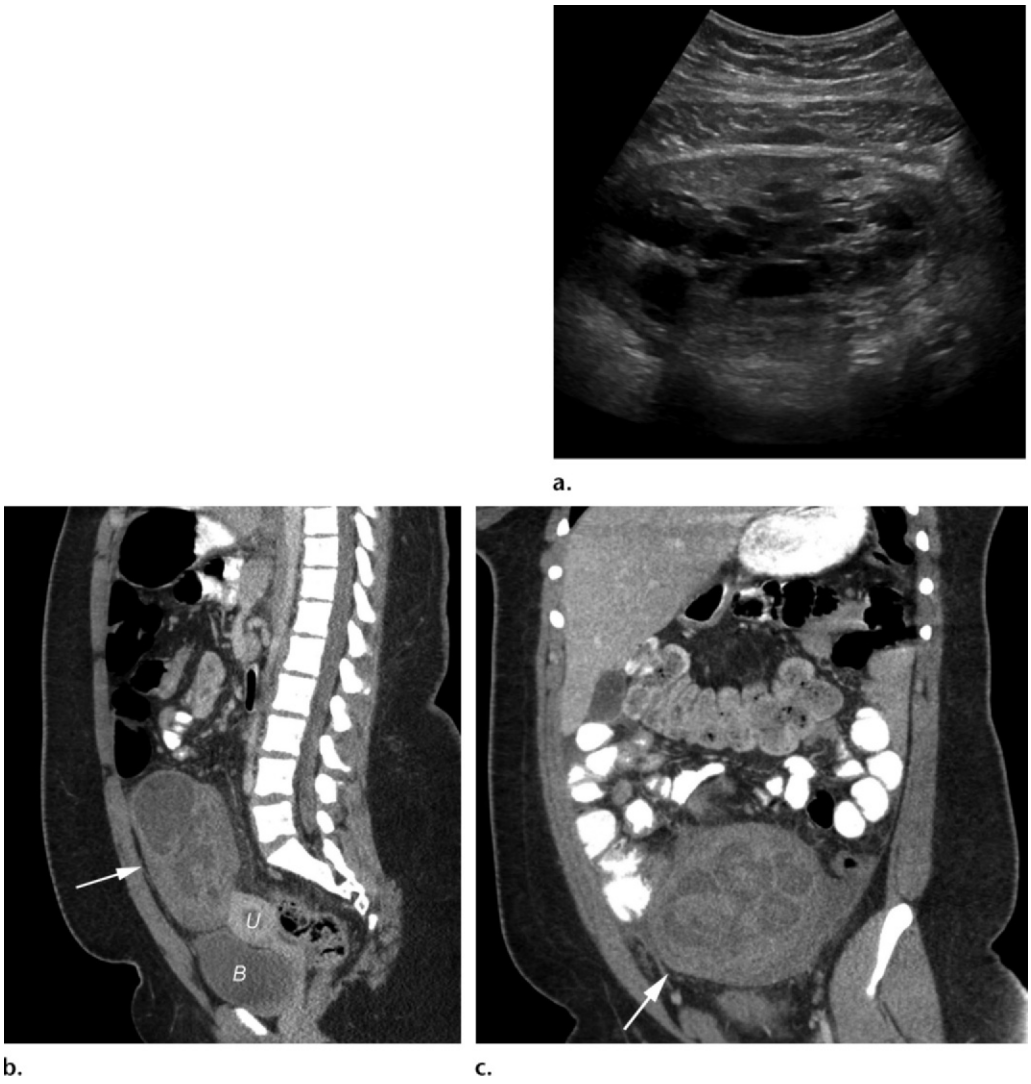

Figure 8. Ovarian torsion in a 14-year-old girl with abdominal pain of 3 days' duration. **(a)** Transverse US image of the pelvis shows an enlarged right ovary with multiple central cysts. **(b, c)** Sagittal **(b)** and coronal **(c)** CT images of the pelvis show a thick-walled mass (arrow) with central areas of low attenuation. At surgery, the mass was found to be a torsed right ovary. Pathologic analysis results confirmed the diagnosis of ovarian torsion with hemorrhagic necrosis. *B* = bladder, *U* = uterus.

status of the child, particularly during puberty (17). Comparing the size of the ovary of concern with the size of the contralateral ovary is key to making an accurate diagnosis of ovarian torsion (2,17). Servaes et al (2) reported a median volume for the torsed ovaries that was 12 times that on the normal contralateral side. Others have indicated that ovarian torsion should be suspected if the ovary is three to 24 times the size of the normal ovary (14). We suggest that torsion should be suspected when the volume is at least three times greater. Linam et al (17) stated that an adnexal volume of 75 mL should increase suspicion for torsion, although they noted that using this criterion could result in a high false-positive rate, particularly if the symptomology was ignored. Otjen et al (34) reported a rare single case of ovarian torsion that manifested without definitive ovarian enlargement but with a change in the ovary's position compared with its position at a prior examination.

Solid Mass with Peripheral Cysts.—A specific US sign described in association with ovarian torsion in adolescents is the presence of multiple follicles at the periphery of a unilaterally enlarged edematous ovary (Figs 5a, 6, 7a) (2,3,30–32). The follicles have been described as spherical and smooth walled (2,30). Follicular diameters have been reported to range from 8–15 mm to 25 mm (2,30,32). The importance of this size is unknown. In the case of torsion, follicular enlargement is thought to be secondary to the transudation of fluid into the follicles due to increased intraovarian pressure as the ovary torses (13,32). High-frequency US can

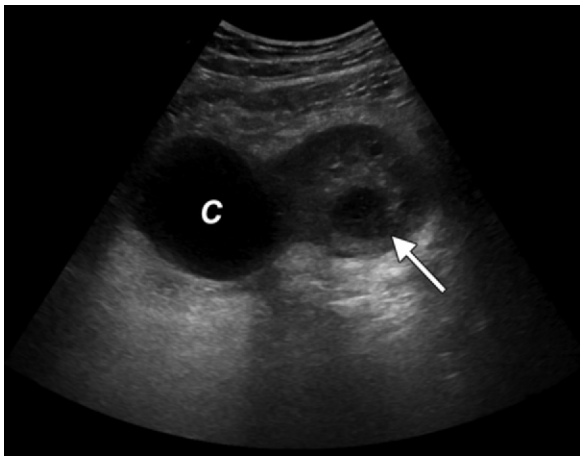

Figure 9. Adnexal torsion in a 13-year-old girl with a right adnexal simple cyst *(C)*. Transverse US image shows that the right ovary is enlarged and has a large debris-containing peripheral follicle (arrow).

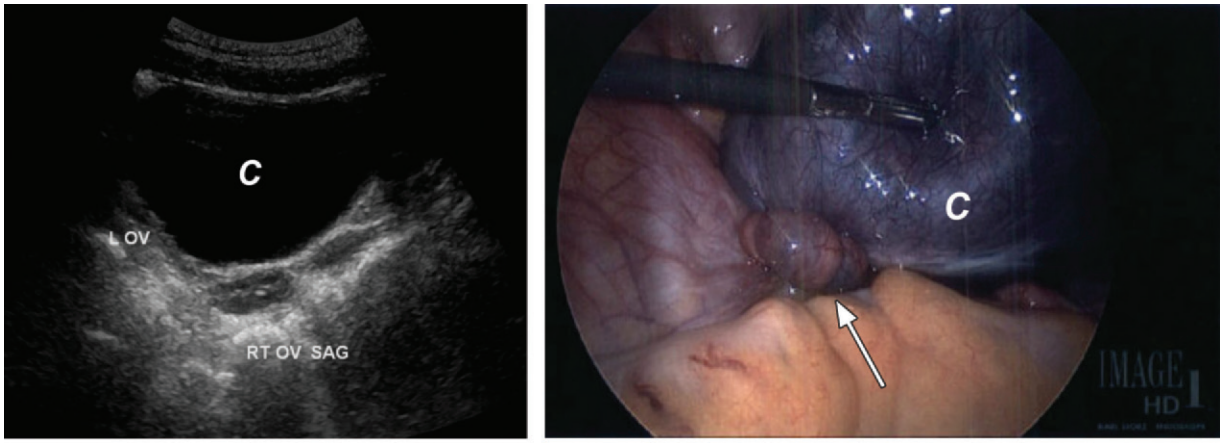

a. **b.**

Figure 10. Adnexal torsion in a 14-year-old girl with left lower quadrant pain. **(a)** Sagittal US image shows a large adnexal cyst *(C)* that has completely replaced the left ovary *(L OV)*. The right ovary *(RT OV)* is normal. The bladder was decompressed by using a Foley catheter (not shown). **(b)** Intraoperative photograph shows a large paratubal cyst *(C)* with torsion of the fallopian tube (arrow).

depict fluid-debris levels in these follicles, which have a reported sensitivity of 85% for the diagnosis of ovarian torsion (32) (Fig 7d). Peripherally located cysts may be seen in the normal ovaries of fertile women and in the setting of polycystic ovarian syndrome. However, the presence of peripheral cysts combined with stromal edema, asymmetric ovarian enlargement, and unilateral pelvic pain favors a diagnosis of ovarian torsion (3,31,32).

Adnexal Masses.—Adnexal masses increase the weight of the ovary and thus theoretically predispose it to torsion (3). In a review of 97 cases of pediatric ovarian torsion, Oltmann et al (4) found an identifiable adnexal mass or cyst in 52 (54%) of the torsed adnexa. Cysts, paratubal and follicular (simple) cysts in particular, were the most common adnexal lesions in the torsed ovaries (4,9,22) (Figs 9, 10). Cysts appear as anechoic round structures with thin, imperceptible walls and increased through transmission.

Benign neoplasms occur in 19% of cases of ovarian torsion, with mature cystic teratoma being the most frequently seen (4,27) (Figs 11, 12). Teratomas appear as heterogeneous masses with both cystic and solid components. The solid echogenic components may represent fat, sebaceous material, hair, and/or calcification from teeth or bone (35). Fat-fluid levels whereby fat floats in a nondependent manner in the cyst may be seen (35). Posterior acoustic shadowing is a characteristic US finding of teratomas, and it may be secondary to calcification, sebum, and/or hair (Fig 11) (13,35,36). The "tip of the iceberg" sign of ovarian teratoma refers to posterior acoustic shadowing that may obscure deeper aspects of the mass (13,35). Adnexal masses in torsed ovaries are almost never malignant (4,22,37). New-onset severe, unilateral pelvic pain in the setting of a known adnexal mass

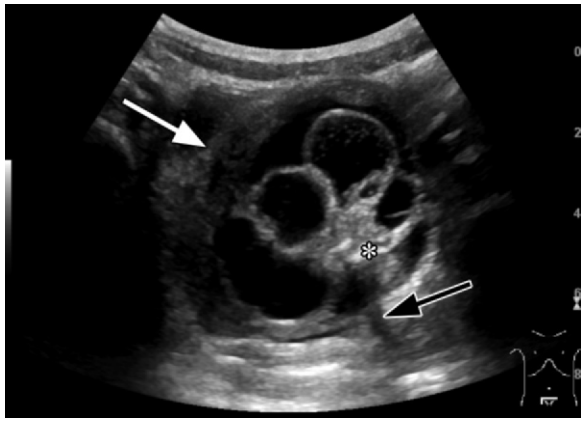

Figure 11. Ovarian torsion with a teratoma in a 5-year-old girl with a 3-day history of right abdominal pain. Transverse US image shows a complex mass (white arrow) that contains multiple round cystic regions and echogenic foci (*) with posterior shadowing (black arrow), which is consistent with calcification or sebaceous material. Torsion was found at surgery.

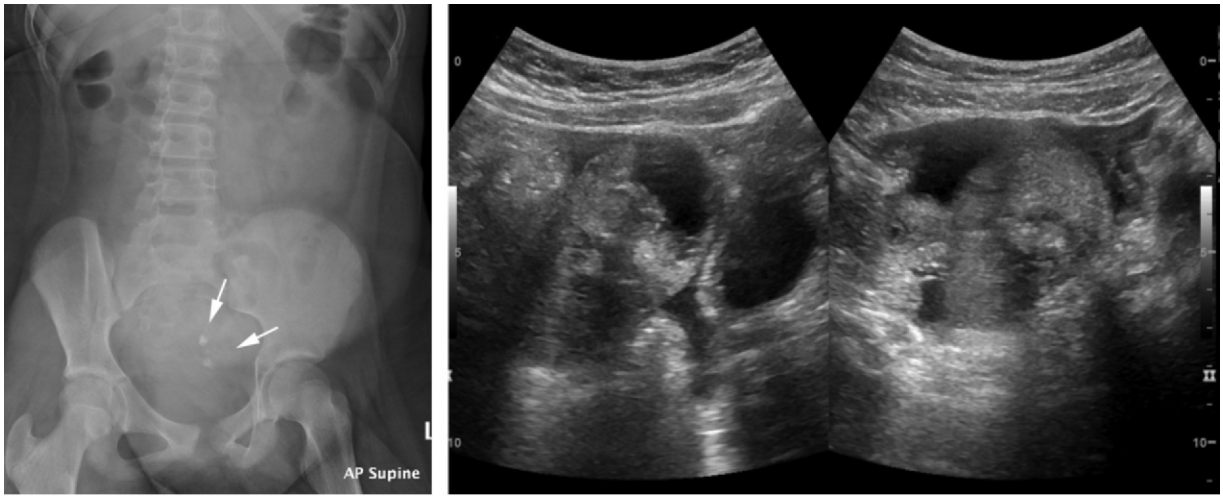

a. b.

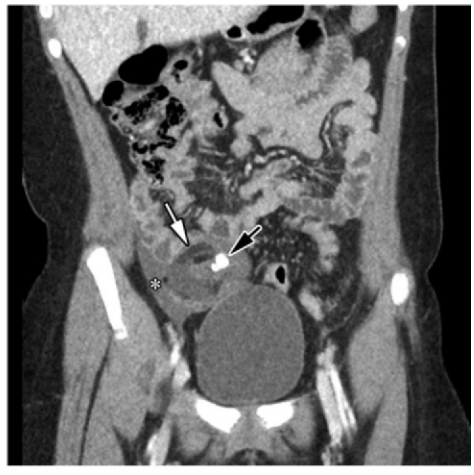

c.

Figure 12. Ovarian torsion with a teratoma in an 11-year-old girl with recurrent episodic lower abdominal pain. **(a)** Anteroposterior abdominal radiograph shows a paucity of bowel gas and several calcifications (arrows) in the pelvis. **(b)** Longitudinal (left) and transverse (right) US images show a heterogeneous adnexal mass with cystic areas, echogenic areas, and areas that shadow. **(c)** Coronal CT image shows a mass in the right pelvis, with low-attenuating fat (white arrow) and high-attenuating calcification (black arrow), consistent with a teratoma. A small amount of free fluid (*) is present in the pelvis. Adnexal torsion with a teratoma was confirmed at surgery.

or cyst, specifically a simple cyst or teratoma, should raise suspicion for ovarian torsion.

Color Doppler US Findings.—Color Doppler US evaluation is not reliable for confirming or excluding ovarian torsion (2,3,17). The absence of arterial and venous flow in the ovary and decreased venous flow are common Doppler US findings of ovarian torsion (37) (Fig 5c). However, these findings are nonspecific, because absent Doppler flow is frequently seen in nontorsed pediatric ovaries (17). Preserved arterial flow may be seen in cases of ovarian torsion—either secondary to lymphatic or venous obstruction producing symptoms before the later development of arterial occlusion, or owing to the dual arterial supply to the ovary from the uterine arteries (13,15). In adults, the twisted vascular pedicle has been described as a specific sign of ovarian torsion and can be seen as a round hyperechoic structure with multiple concentric hypoechoic stripes on transvaginal US images (17,28). However, this sign is less

Table 2: Imaging Patterns of Ovarian Torsion in Fetuses and Neonates

Cyst with a fluid-debris level
Double wall sign
Cyst with a retracting clot
Cystic mass with meshlike septa
Calcifications in the cyst wall
US appearance that evolves over time
Round soft-tissue opacity on radiographs
Varying position on radiographs

reliable in the pediatric population, as imaging in children is almost always performed by using the transabdominal approach (17,28).

Imaging Patterns in Fetuses and Neonates

Ovarian torsion in fetuses and neonates can occur in the setting of a large ovarian cyst that may predispose the ovary to torse. Ovarian cysts are the most common cystic abdominal masses in female fetuses and have an incidence of approximately one in 2500–2625 pregnancies/live births (38,39). Fetal ovarian cysts occur in the late 2nd trimester and 3rd trimester and are secondary to elevated maternal and placental hormone levels (40,41). Most of these cysts resolve spontaneously; however, 5-cm or larger cysts are associated with an increased risk of torsion (23,24,42). Torsion usually occurs antenatally and is clinically silent (10,43). In the neonate, however, torsion may be, but only rarely is associated with vomiting, fever, or leukocystosis (10,43). In utero ovarian torsion is normally discovered at routine follow-up obstetric US imaging, where a previously seen simple ovarian cyst has developed complex features (24,25).

Ovarian torsion in the fetus or neonate has a more variable appearance on gray-scale US images than does that seen in children and adolescents with acute pain. This is because neonatal ovarian torsion is usually the result of an older antenatal torsion. When imaging is performed in a neonate, hemorrhagic necrosis from the antenatal torsion may have developed and thus may cause a more heterogeneous-appearing ovary. Complex cystic changes within the necrotic ovary, fluid-debris levels, and either evidence of a retractile clot or the reticular echogenicity of an old hemorrhage can be seen (2,10,44–46).

Several US patterns of neonatal ovarian torsion have been described and include a cyst with a fluid-debris level, the "double wall" sign, a cyst with a retracting clot, and a cyst with multiple meshlike septa (10,46) (Table 2). A fluid-debris level in an ovarian cyst is a specific sign of ovarian torsion in neonates and secondary to cyst fluid separating from a liquefied hematoma (10,46,47) (Fig 13). The double wall sign has been described in the setting of neonatal ovarian torsion as a cyst with an echogenic inner wall and hypoechoic rim (46) (Fig 13). In addition, a cyst with a retractile clot, seen as a heterogeneous nodule capped by a crescent-shaped rim of anechoic fluid, also has been reported in cases of neonatal ovarian torsion (10) (Fig 14). A cyst with multiple meshlike septa, seen as echogenic fine lines that traverse the cyst, also has been described (10,42,44,46) (Fig 15, 16a). Increased echogenicity of the cyst wall, which may represent calcification, has been associated with ovarian infarction (10,46,48) (Fig 13b).

A change in the appearance of a cyst from simple to complex on subsequently obtained obstetric US images should increase suspicion for in utero ovarian torsion (24,25) (Fig 17). On postnatal radiographs, a torsed ovary may appear as a round soft-tissue opacity in the abdomen or pelvis, with or without a thin rim of calcification (46) (Fig 13a). A change in the location of a soft-tissue mass seen on a subsequently obtained abdominal radiograph suggests that the mass is attached to a pedicle. When this change is seen in a female neonate, ovarian torsion should be considered (Fig 16b, 16c). Autoamputation of a torsed ovary is demonstrated by a highly mobile soft-tissue mass with peripheral calcification (10,23,46,48).

CT and MR Imaging

CT and MR imaging are used as secondary imaging examinations in the diagnosis of ovarian torsion. The advantage of CT is that it can be performed in the acute setting. However, unlike US, it exposes children to ionizing radiation. The findings of ovarian torsion at CT have been described in several studies (3,27,49). These findings include an enlarged adnexal mass that may be midline or on the contralateral side of the pelvis, a cystic appearance of the torsed ovary, deviation of the uterus to the side of the torsed ovary, and thickening of the fallopian tube (27,49). Peripherally located follicles with an edematous ovarian stroma, poor enhancement of the ovary, adnexal hemorrhage, heterogeneity and increased attenuation of the surrounding fat, plasma erythrocyte levels within the torsed ovary, and/or a twisted vascular pedicle also may be seen (3,27,49,50) (Figs 4b, 7b, 8b, 8c).

In contrast, MR imaging does not involve the use of ionizing radiation. However, owing to its cost and restricted availability, this examination may be of limited use in emergent situations.

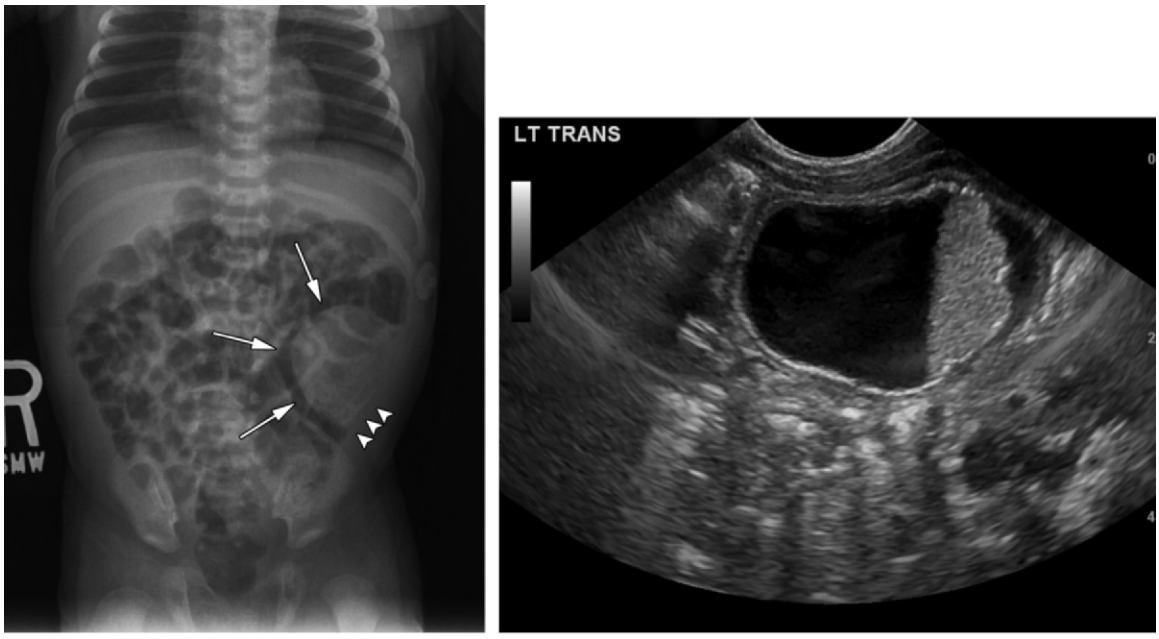

a. b.

Figure 13. In utero ovarian torsion in an 11-day-old infant who presented with fussiness. **(a)** Frontal abdominal radiograph shows a round soft-tissue mass (arrows) in the lower left region of the abdomen, superior to the pelvis. Calcification (arrowheads) is seen at the periphery of the mass. **(b)** Transverse US image shows a cystic mass with a fluid-debris level, in the left abdominal region. A double wall sign—that is, an echogenic inner wall and hypoechoic outer wall—is present. The highly echogenic inner wall suggests calcification, which was confirmed on the radiograph.

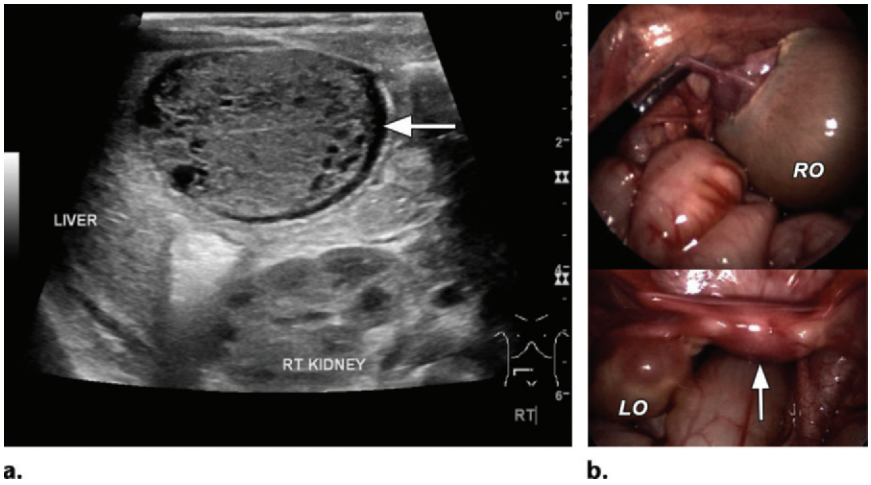

a. b.

Figure 14. Ovarian torsion in a 3-month-old infant. **(a)** Transverse US image shows a right upper quadrant heterogeneous mass, consistent with a clot, in a necrotic torsed ovary. The fluid (arrow) at the periphery of the mass suggests that the clot is retractile. **(b)** Intraoperative photographs show an enlarged dusky right ovary *(RO)* and a normal left ovary *(LO)* and uterus (arrow).

MR images may show ovarian enlargement with a central afollicular region secondary to hemorrhage and edema, as well as peripherally located follicles (50,51). These findings are best seen on T2-weighted MR images without fat suppression (27,50). Fat-suppressed T1-weighted MR imaging may aid in the detection of hemorrhage, and contrast-enhanced fat-suppessed T1-weighted MR imaging can depict poor enhancement of the ovary, which suggests infarction or necrosis (3,50). Contrast-enhanced MR imaging may also aid in detecting the swirling appearance of a twisted pedicle (50). In neonates, a fluid-debris level also may be seen on MR images.

Differential Diagnoses

Several entities may simulate torsed ovaries. In the adolescent population, hemorrhagic cysts may have an appearance similar to that of torsed ovaries (44). These cysts may appear

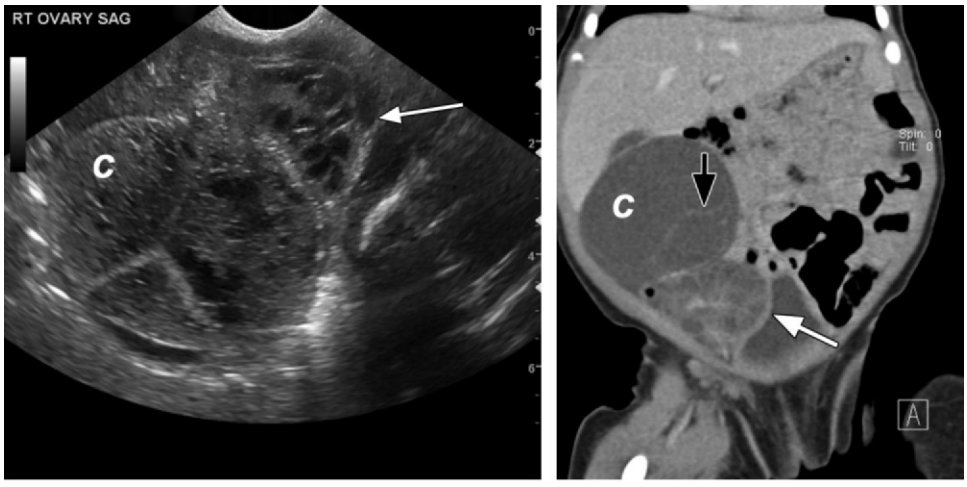

a. b.

Figure 15. Neonatal ovarian torsion in a 2-day-old infant with a prenatally diagnosed mass. The mass was surgically confirmed to be due to left ovarian torsion with a complex adnexal cyst. **(a)** Sagittal US image shows a complex cyst *(C)* with thick meshlike septa and multiple echogenic reticulations, consistent with evolving hemorrhage. The left ovary (arrow) with multiple dilated follicles is seen in the right pelvis. **(b)** Coronal CT image shows a large complex cyst *(C)* with a thin septum (black arrow). Inferiorly and to the left, a cystic-appearing left ovary (white arrow) contains multiple enlarged follicles. The patient underwent cystectomy and detorsion.

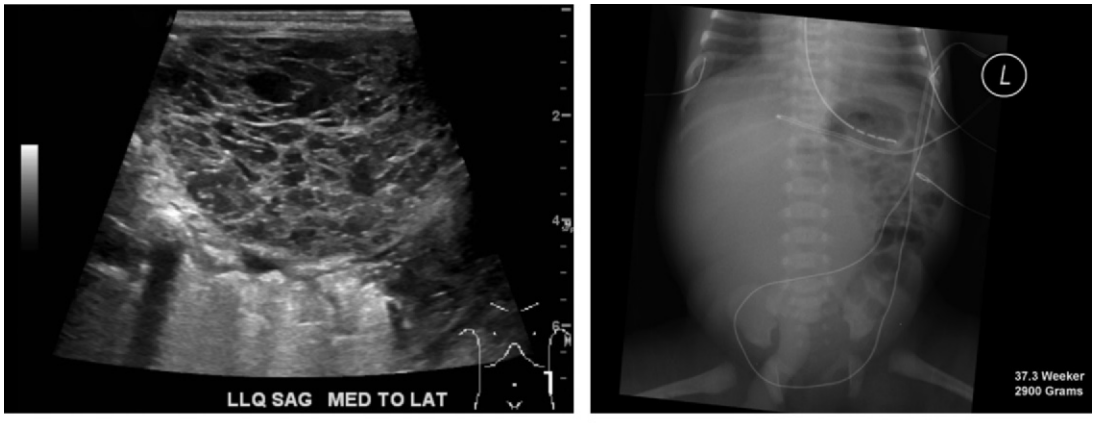

a. b.

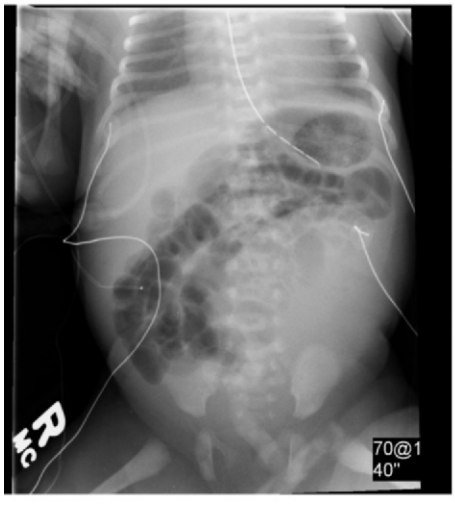

c.

Figure 16. Neonatal ovarian torsion. **(a)** Lower left quadrant sagittal US image obtained in a 1-day-old infant shows a complex multicystic mass with meshlike areas of reticulation. **(b)** Frontal radiograph obtained in the same patient at birth shows a large mass in the right abdomen, with displacement of the bowel to the left. **(c)** Frontal radiograph obtained in the same patient at 12 hours of life shows that the mass is now in the left abdomen; this suggests that the mass is on a pedicle and is ovarian in origin. A torsed right ovary was found at surgery. This is an example of how prominent masses originating in pelvic organs can rise from the small fetal or neonatal pelvis and move into the lower region of the abdomen.

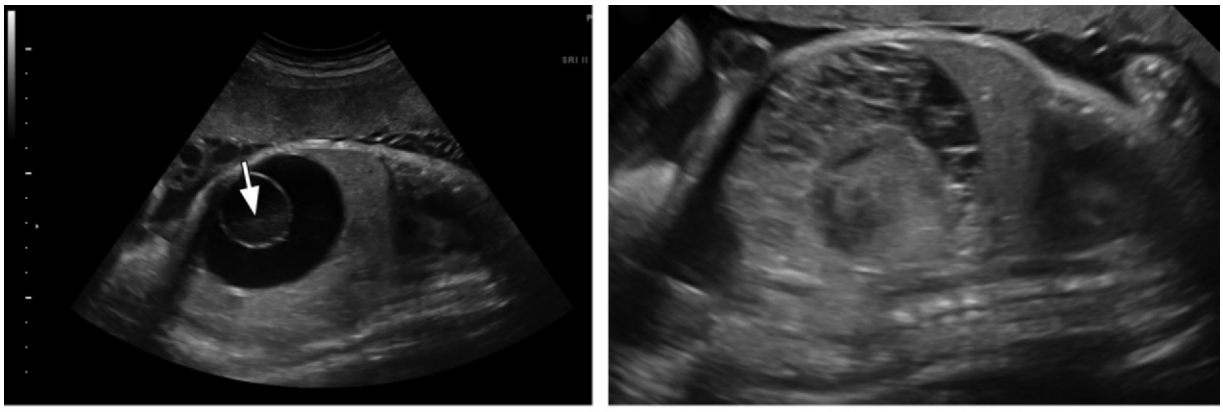

a. b.

Figure 17. In utero ovarian torsion with a cyst that evolved in appearance over time. Prenatal US images obtained at 34 **(a)** and 37 **(b)** weeks gestation show a fluid-debris level (arrow in **a**) within a cyst abdominopelvic mass. The presence of a daughter cyst suggests that the cystic mass is of ovarian origin. The fluid-debris level suggests the presence of hemorrhage with torsion. At 37 weeks **(b)**, a solid cystic mass with areas of meshlike septa is present and suggests the further development of hemorrhage and the intrauterine development of ovarian torsion, which were proven at surgery.

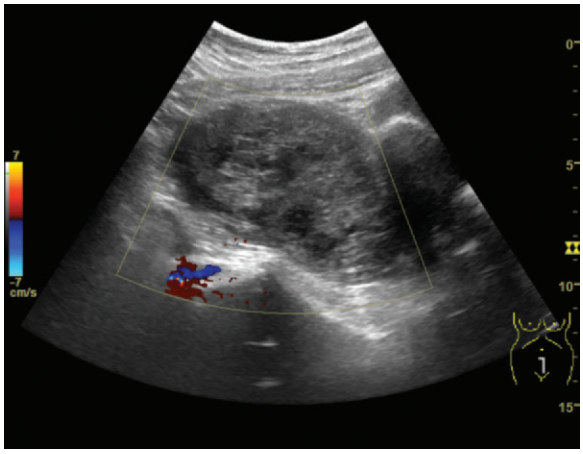

Figure 18. Hemorrhagic ovarian cyst in a 15-year-old girl who had acute abdominal pain for 1 day. Sagittal color Doppler US image shows an enlarged solid-appearing ovary with no definitive flow. At surgery, a hemorrhagic cyst was found without torsion of the ovary. Large hemorrhagic cysts can simulate torsed ovaries at US.

Figure 19. Yolk sac tumor in a 14-year-old girl with chronic back pain. Lower left quadrant sagittal US image of the pelvis shows an enlarged, mixed solid and cystic mass with several round anechoic foci. Pathologic analysis results proved this mass to be a yolk sac tumor.

echogenic during their acute stage, and affected patients may present with severe abdominal pain (Fig 18). A retractile clot or reticular pattern of internal echoes may appear as the blood by-products of the hemorrhagic cyst evolve. Tubo-ovarian abscess and ovarian neoplasms also may manifest with pain and as heterogeneous adnexal masses, which may resemble ovarian torsion at US (Fig 19).

In neonates, any complex cystic mass can simulate a torsed ovary. Owing to the highly variable US appearance of neonatal ovarian torsion, distinguishing it from other complex cystic masses seen in female neonates can be challenging. Hematocolpos, duplication cysts, urachal remnants, meconium pseudocysts, and lymphatic malformations can have US features that resemble those of neonatal ovarian torsion. The differentiation of these entities can be helpful in deciding whether to proceed with surgical versus conservative management. A finding that is helpful in determining the ovarian origin of a cystic mass is the "daughter cyst" sign (41,52,53). A daughter cyst is a round anechoic structure abutting the wall of the ovarian cyst (52).

Hematocolpos refers to vaginal dilatation secondary to outlet obstruction caused by an imperforate hymen, a transverse vaginal septum, vaginal agenesis, or vaginal atresia (13,41). On US images, a tubular fluid-filled mass is seen between the bladder and the rectum, representing a vagina distended with fluid (13). Echogenic debris may be seen layering dependently, representing cellular debris or blood (13) (Fig 20). Hematocolpos may

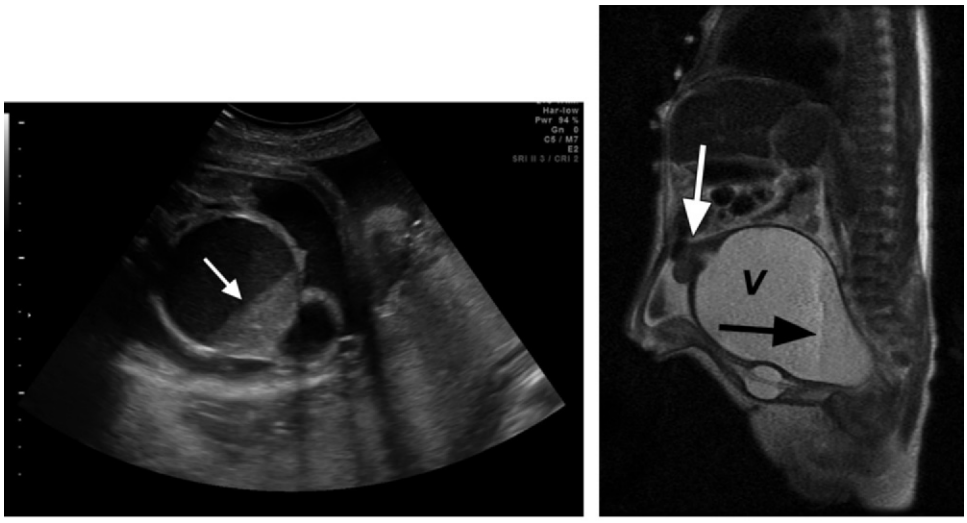

a. b.

Figure 20. Hematocolpos. **(a)** Prenatal US image shows a midline cystic mass with a fluid-debris level (arrow). **(b)** Sagittal postnatal MR image (from the case in **a**) shows a fluid-debris level (black arrow) in a markedly dilated vagina *(V)*. The white arrow points to the uterus.

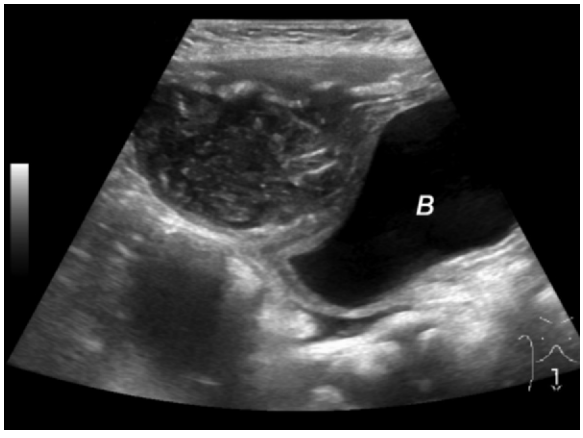

Figure 21. Infected urachal remnant in an 11-month-old infant with abdominal pain for 1 day. Sagittal US image shows a complex cystic structure near the bladder *(B)* apex.

be diagnosed by identifying the midline location between the bladder and the rectum. Also, the uterus can be seen superior to the dilated vagina.

Duplication cysts are congenital abnormalities that can be found anywhere along the gastrointestinal tract, but they most commonly involve the ileum (54). At imaging, these cysts typically appear as unilocular cystic masses. However, they may have internal echoes, debris, septa, and/or wall thickening if there is accompanying infection or hemorrhage (54,55). The double wall sign has been classically described as a finding of enteric duplication cysts and represents the inner echogenic mucosa and the outer hypoechoic submucosal layer (44,54,55). These imaging findings may simulate those of a complex cyst seen with neonatal ovarian torsion.

Urachal remnants develop when the channel that allows communication between the bladder and the anterior abdominal wall during fetal life fails to obliterate. Urachal remnants may have a complex appearance, with multiple internal echoes, on US images when they become infected. However, they can be distinguished from neonatal ovarian torsion owing to the anterior midline location of the infected urachal remnant at the apex of the bladder (Fig 21).

Meconium pseudocysts can form as a complication of meconium peritonitis that results from in utero bowel perforation. Meconium pseudocysts are complex-appearing masses with echogenic contents. They may appear walled off or conform to the peritoneal cavity. The walls of meconium pseudocysts may be highly echogenic at US owing to calcifications.

Lymphatic malformations are benign tumors, hypothesized to have developed as a result of the embryologic failure of ectopic lymphatic tissue in establishing a normal communication with the remainder of the lymphatic system (41). On US images, lymphatic malformations appear as thin-walled multiloculated masses with thin septa (41). These masses contain fluid that is usually anechoic but may become more echogenic when there is accompanying infection or hemorrhage.

Management of Pediatric Ovarian Torsion

In the pediatric population, in which ovarian torsion usually presents acutely, management

is performed with the goal of preserving ovarian tissue. Acute ovarian torsion is treated with emergent laparoscopic surgical detorsion and visual inspection of the ovary for viability (56). Adnexal torsion has historically been treated with oophorectomy owing to fear of a pulmonary embolus developing from the torsed pedicle (1). The results of several studies have shown that conservative surgery rather than oophorectomy is the preferred technique, allowing preservation of ovarian function (57). Salpingo-oophorectomy is usually reserved for cases in which the ovary is frankly necrotic—that is, black, gelatinous, small, and with loss of normal anatomic structure (56). However, study results have shown that even ovaries that appear black or blue retain function after detorsion (56). In some studies conducted with follow-up US, there has been normal follicular development in torsed ovaries that appeared blue or black at surgery (56).

If a cyst is seen at inspection of the ovary after detorsion, then cystectomy, cyst fenestration, or cyst aspiration can be performed (56). Masses that raise concern for malignancy are treated with salpingo-oophorectomy (56). Performing oophoropexy after detorsion is controversial, with some advocating this procedure in the pediatric population, particularly after loss of the contralateral ovary or with recurrent intermittent torsion (4,56). However, others have concerns about the patient's future fertility after oophoropexy, since long-term studies of this outcome aspect have not been performed.

In the fetal and neonatal population, management is more controversial. Ovarian torsion in this population usually occurs in association with an underlying cyst (58). Although approximately 50% of prenatally detected cysts regress spontaneously, 35% of them develop in association with complications such as ovarian torsion and hemorrhage (59). In addition, while cysts smaller than 5 cm tend to regress, those 5 cm or larger involve a greater risk for torsion (23,24,42,59). Because torsion occurs antenatally more commonly than it does neonatally, some authors (24,60,61) believe that simple ovarian cysts should be decompressed by means of in utero aspiration to prevent future torsion. Bagolan et al (24) reported that 86% of simple cysts larger than 5 cm resolved after prenatal aspiration, with no need for postnatal surgical intervention. Among the patients with cysts larger than 5 cm who did not undergo aspiration, only 15% of the cysts resolved, while 85% of them remained and became complicated by torsion requiring postnatal oophorectomy (24). Although study results (24,59,61) have shown prenatal aspiration to be safe and effective, it is rarely performed (59). This may be due to a lack of experience performing the procedure, the lack of controlled trials, and concerns about potential complications such as cyst rupture and peritonitis (41,58,59).

Many authors (58,59) advocate prenatal US observation of fetal ovarian cysts. Small simple cysts tend to involute by the time the child reaches 1 year of age (62). Historically, when the cyst persisted at postnatal follow-up imaging, measured 4–5 cm, increased in size, or developed complex features at US, conservative surgery with cystectomy or cyst fenestration has been performed in an attempt to preserve the ovary and fertility (58,62). However, in many cases, the cyst is intimately associated with the underlying ovarian parenchyma, precluding the use of conservative surgical approaches such as cystectomy or fenestration, and oophorectomy or salpingo-oophorectomy is required (58,62).

Minimally invasive techniques have been used to manage simple ovarian cysts during the neonatal period, with improved salvage rates compared with those achieved when the cysts were treated with surgery (58,62,63). In a study by Kessler et al (58), US-guided aspiration of simple cysts larger than 4 cm performed during the neonatal period led to ovarian preservation in 59% of cases, while surgery enabled the ovary to be salvaged in only 25% of cases. Cho et al (63) support performing laparoscopic aspiration owing to the possible difficulty in avoiding adjacent organs at US-guided aspiration and the ability to better assess ovarian viability at laparoscopy.

In the treatment of complex ovarian cysts that may have been associated with in utero torsion, traditional management involves surgery with cystectomy or oophorectomy, if needed. Some authors advocate performing US-guided or laparascopic aspiration of complex cysts (58,63). In a study by Enriquez et al (38), complex ovarian cysts were managed conservatively with clinical and US monitoring and found to have involuted spontaneously by the time the child reached 1 year of age. Therefore, they propose that surgical management of complex ovarian cysts should be pursued only in cases of very large cysts that cause clinical symptoms or do not regress spontaneously (38).

Conclusion

Several imaging findings of ovarian torsion have been described, although no one sign is characteristic of torsion. The most commonly seen finding of ovarian torsion is asymmetric enlargement of one ovary in the setting of acute

abdominal pain. Peripherally located follicles are a specific sign of torsion in children and adolescents. Adnexal cysts or masses may be present. Doppler US has limited use in the evaluation of ovarian torsion, and the presence of Doppler flow in an ovary does not exclude torsion. During the perinatal period, a fluid-debris level in the ovary is a frequently seen sign of torsion. For the radiologist, both the clinical history and the imaging information are necessary to make an accurate diagnosis of ovarian torsion.

Acknowledgments.—The authors thank Drs Max Langham and Eunice Huang of the Department of Pediatric Surgery, LeBonheur Children's Hospital, for the intraoperative images; and Kimberly Bomar, Maria Centeno, Amy Huffman, Andrea LaFaver, Apprecia Lee, Leah McQuilliams, Danielle Smaili, and Ashton Underwood for their US expertise.

References

1. Descargues G, Tinlot-Mauger F, Gravier A, Lemoine JP, Marpeau L. Adnexal torsion: a report on forty-five cases. Eur J Obstet Gynecol Reprod Biol 2001;98(1):91–96.
2. Servaes S, Zurakowski D, Laufer MR, Feins N, Chow JS. Sonographic findings of ovarian torsion in children. Pediatr Radiol 2007;37(5):446–451.
3. Ngo AV, Otjen JP, Parisi MT, Ferguson MR, Otto RK, Stanescu AL. Pediatric ovarian torsion: a pictorial review. Pediatr Radiol 2015;45(12):1845–1855; quiz 1842–1844.
4. Oltmann SC, Fischer A, Barber R, Huang R, Hicks B, Garcia N. Cannot exclude torsion: a 15-year review. J Pediatr Surg 2009;44(6):1212–1216; discussion 1217.
5. Laufer MR, Goldstein DP. Gynecologic pain: dysmenorrhea, acute and chronic pelvic pain, endometriosis, and premenstrual syndrome. In: Emans J, Laufer MR, Goldstein DP, eds. Pediatric and adolescent gynecology. 5th ed. Philadelphia, Pa: Lippincott, Williams & Wilkins, 2005; 417–469.
6. Cohen HL, Safriel YI. Ovarian torsion. In: Cohen HL, Sivit CJ, eds. Fetal and pediatric ultrasound: a casebook approach. New York, NY: McGraw-Hill, 2001; 516–519.
7. Gross M, Blumstein SL, Chow LC. Isolated fallopian tube torsion: a rare twist on a common theme. AJR Am J Roentgenol 2005;185(6):1590–1592.
8. Helvie MA, Silver TM. Ovarian torsion: sonographic evaluation. J Clin Ultrasound 1989;17(5):327–332.
9. Kokoska ER, Keller MS, Weber TR. Acute ovarian torsion in children. Am J Surg 2000;180(6):462–465.
10. Nussbaum AR, Sanders RC, Hartman DS, Dudgeon DL, Parmley TH. Neonatal ovarian cysts: sonographic-pathologic correlation. Radiology 1988;168(3):817–821.
11. Moore KL, Persaud TV, Torchia MG. Urogenital system. In: Moore KL, ed. The developing human. 10th ed. Philadelphia, Pa: Saunders/Elsevier, 2015; 241–282.
12. Laufer MR, Goldstein DP. Benign and malignant ovarian masses. In: Emans J, Laufer MR, Goldstein DP, eds. Pediatric and adolescent gynecology. 5th ed. Philadelphia, Pa: Lippincott, Williams & Wilkins, 2005; 685–725.
13. Siegel MJ. Female pelvis. In: Siegel MJ, ed. Pediatric sonography. 4th ed. Philadelphia, Pa: Lippincott, Williams & Wilkins, 2011; 509–553.
14. Cohen HL. Abnormalities of the female genital tract. In: Slovis TL, ed. Caffey's pediatric diagnostic imaging. 11th ed. St Louis, Mo: Mosby, 2008; 2428–2455.
15. Standring S. Female reproductive system. In: Standring S, ed. Gray's anatomy. 41st ed. Philadelphia, Pa: Elsevier, 2016; 1288–1313.
16. Cohen HL, Eisenberg P, Mandel F, Haller JO. Ovarian cysts are common in premenarchal girls: a sonographic study of 101 children 2-12 years old. AJR Am J Roentgenol 1992;159(1):89–91.
17. Linam LE, Darolia R, Naffaa LN, et al. US findings of adnexal torsion in children and adolescents: size really does matter. Pediatr Radiol 2007;37(10):1013–1019.
18. Langer JE, Oliver ER, Lev-Toaff AS, Coleman BG. Imaging of the female pelvis through the life cycle. RadioGraphics 2012;32(6):1575–1597.
19. Cohen HL, Gale B. Neonatal ovarian torsion. In: Cohen HL, Sivit CJ, eds. Fetal and pediatric ultrasound: a casebook approach. New York, NY: McGraw-Hill, 2001; 482–485.
20. Cohen HL, Shapiro MA, Mandel FS, Shapiro ML. Normal ovaries in neonates and infants: a sonographic study of 77 patients 1 day to 24 months old. AJR Am J Roentgenol 1993;160(3):583–586.
21. Farrell TP, Boal DK, Teele RL, Ballantine TV. Acute torsion of normal uterine adnexa in children: sonographic demonstration. AJR Am J Roentgenol 1982;139(6):1223–1225.
22. Cass DL. Ovarian torsion. Semin Pediatr Surg 2005;14(2):86–92.
23. Ozcan HN, Balci S, Ekinci S, et al. Imaging findings of fetal-neonatal ovarian cysts complicated with ovarian torsion and autoamputation. AJR Am J Roentgenol 2015;205(1):185–189.
24. Bagolan P, Giorlandino C, Nahom A, et al. The management of fetal ovarian cysts. J Pediatr Surg 2002;37(1):25–30.
25. Galinier P, Carfagna L, Juricic M, et al. Fetal ovarian cysts management and ovarian prognosis: a report of 82 cases. J Pediatr Surg 2008;43(11):2004–2009.
26. Garel L, Dubois J, Grignon A, Filiatrault D, Van Vliet G. US of the pediatric female pelvis: a clinical perspective. RadioGraphics 2001;21(6):1393–1407.
27. Chang HC, Bhatt S, Dogra VS. Pearls and pitfalls in diagnosis of ovarian torsion. RadioGraphics 2008;28(5):1355–1368.
28. Lee EJ, Kwon HC, Joo HJ, Suh JH, Fleischer AC. Diagnosis of ovarian torsion with color Doppler sonography: depiction of twisted vascular pedicle. J Ultrasound Med 1998;17(2):83–89.
29. Quillin SP, Siegel MJ. Transabdominal color Doppler ultrasonography of the painful adolescent ovary. J Ultrasound Med 1994;13(7):549–555.
30. Graif M, Shalev J, Strauss S, Engelberg S, Mashiach S, Itzchak Y. Torsion of the ovary: sonographic features. AJR Am J Roentgenol 1984;143(6):1331–1334.
31. Graif M, Itzchak Y. Sonographic evaluation of ovarian torsion in childhood and adolescence. AJR Am J Roentgenol 1988;150(3):647–649.
32. Kiechl-Kohlendorfer U, Maurer K, Unsinn KM, Gassner I. Fluid-debris level in follicular cysts: a pathognomonic sign of ovarian torsion. Pediatr Radiol 2006;36(5):421–425.
33. Cohen HL, Tice HM, Mandel FS. Ovarian volumes measured by US: bigger than we think. Radiology 1990;177(1):189–192.
34. Otjen JP, Stanescu L, Goldin A, Parisi MT. A normal ovary in an abnormal location: a case of torsion. J Clin Ultrasound 2015;43(9):578–580.
35. Cohen HL, Safriel YI. Benign cystic teratomas of the ovary. In: Cohen HL, Sivit CJ, eds. Fetal and pediatric ultrasound: a casebook approach. New York, NY: McGraw-Hill, 2001; 506–510.
36. Heo SH, Kim JW, Shin SS, et al. Review of ovarian tumors in children and adolescents: radiologic-pathologic correlation. RadioGraphics 2014;34(7):2039–2055.
37. Albayram F, Hamper UM. Ovarian and adnexal torsion: spectrum of sonographic findings with pathologic correlation. J Ultrasound Med 2001;20(10):1083–1089.
38. Enriquez G, Durán C, Torán N, et al. Conservative versus surgical treatment for complex neonatal ovarian cysts: outcomes study. AJR Am J Roentgenol 2005;185(2):501–508.
39. Papic JC, Billmire DF, Rescorla FJ, Finnell SM, Leys CM. Management of neonatal ovarian cysts and its effect on ovarian preservation. J Pediatr Surg 2014;49(6):990–993; discussion 993–994.

40. Sheth R, Hoelzer D, Scattergood E, Germaine P. In utero fetal ovarian torsion with imaging findings on ultrasound and MRI. Case Rep Radiol 2012;2012:151020.
41. Trinh TW, Kennedy AM. Fetal ovarian cysts: review of imaging spectrum, differential diagnosis, management, and outcome. RadioGraphics 2015;35(2):621–635.
42. Garel L, Filiatrault D, Brandt M, et al. Antenatal diagnosis of ovarian cysts: natural history and therapeutic implications. Pediatr Radiol 1991;21(3):182–184.
43. Schmahmann S, Haller JO. Neonatal ovarian cysts: pathogenesis, diagnosis and management. Pediatr Radiol 1997;27(2):101–105.
44. Jain KA. Sonographic spectrum of hemorrhagic ovarian cysts. J Ultrasound Med 2002;21(8):879–886.
45. Laing FC, Allison SJ. US of the ovary and adnexa: to worry or not to worry? RadioGraphics 2012;32(6):1621–1639; discussion 1640–1642.
46. Kim HS, Yoo SY, Cha MJ, Kim JH, Jeon TY, Kim WK. Diagnosis of neonatal ovarian torsion: emphasis on prenatal and postnatal sonographic findings. J Clin Ultrasound 2016;44(5):290–297.
47. Stark JE, Siegel MJ. Ovarian torsion in prepubertal and pubertal girls: sonographic findings. AJR Am J Roentgenol 1994;163(6):1479–1482.
48. Currarino G, Rutledge JC. Ovarian torsion and amputation resulting in partially calcified, pedunculated cystic mass. Pediatr Radiol 1989;19(6-7):395–399.
49. Hiller N, Appelbaum L, Simanovsky N, Lev-Sagi A, Aharoni D, Sella T. CT features of adnexal torsion. AJR Am J Roentgenol 2007;189(1):124–129.
50. Duigenan S, Oliva E, Lee SI. Ovarian torsion: diagnostic features on CT and MRI with pathologic correlation. AJR Am J Roentgenol 2012;198(2):W122–W131.
51. Cheng KL, Tsao TF. Ovarian torsion: appearance on MRI. Pediatr Radiol 2010;40(suppl 1):S104.
52. Lee HJ, Woo SK, Kim JS, Suh SJ. "Daughter cyst" sign: a sonographic finding of ovarian cyst in neonates, infants, and young children. AJR Am J Roentgenol 2000;174(4):1013–1015.
53. Quarello E, Gorincour G, Merrot T, Boubli L, D'Ercole C. The 'daughter cyst sign': a sonographic clue to the diagnosis of fetal ovarian cyst. Ultrasound Obstet Gynecol 2003;22(4):433–434.
54. Macpherson RI. Gastrointestinal tract duplications: clinical, pathologic, etiologic, and radiologic considerations. RadioGraphics 1993;13(5):1063–1080.
55. Godfrey H, Abernethy L, Boothroyd A. Torsion of an ovarian cyst mimicking enteric duplication cyst on transabdominal ultrasound: two cases. Pediatr Radiol 1998;28(3):171–173.
56. Laufer MR. Ovarian and fallopian tube torsion. UpToDate website. https://www.uptodate.com/contents/ovarian-and-fallopan-tube-torsion. Accessed June 18, 2017.
57. Childress KJ, Dietrich JE. Pediatric ovarian torsion. Surg Clin North Am 2017;97(1):209–221.
58. Kessler A, Nagar H, Graif M, et al. Percutaneous drainage as the treatment of choice for neonatal ovarian cysts. Pediatr Radiol 2006;36(9):954–958.
59. Słodki M, Respondek-Liberska M. Fetal ovarian cysts: 420 cases from literature—metaanalysis 1984-2005 [in Polish]. Ginekol Pol 2007;78(4):324–328.
60. Brandt ML, Luks FI, Filiatrault D, Garel L, Desjardins JG, Youssef S. Surgical indications in antenatally diagnosed ovarian cysts. J Pediatr Surg 1991;26(3):276–281; discussion 281–282.
61. Crombleholme TM, Craigo SD, Garmel S, D'Alton ME. Fetal ovarian cyst decompression to prevent torsion. J Pediatr Surg 1997;32(10):1447–1449.
62. Akın MA, Akın L, Özbek S, et al. Fetal-neonatal ovarian cysts: their monitoring and management—retrospective evaluation of 20 cases and review of the literature. J Clin Res Pediatr Endocrinol 2010;2(1):28–33.
63. Cho MJ, Kim DY, Kim SC. Ovarian cyst aspiration in the neonate: minimally invasive surgery. J Pediatr Adolesc Gynecol 2015;28(5):348–353.